Nanoscale Advances

ROYAL SOCIETY OF CHEMISTRY

PAPER

View Article Online
View Journal | View Issue

Cite this: *Nanoscale Adv.*, 2025, **7**, 800

Enhanced photocatalytic performance of polyaniline nanoparticles for efficient dye degradation under simulated sunlight

Chinh Van Tran,†[a] Duy Van Lai,†[ab] Thu Minh Nguyen,[b] Xuan Quynh Thi Le,[b] Hanh Hong Nguyen,[c] Nguyet Thi Minh Quan,[e] Tung Thanh Nguyen[bd] and Duong Duc La*[a]

This study investigates the effectiveness of polyaniline oxide (PANI) nanoparticles as photocatalysts for the degradation of organic dyes under visible light irradiation. Known for their stability and adjustable conductivity, PANI nanoparticles were synthesized *via* a hydrothermal method using P123 surfactants, followed by calcination. The morphology, structural phase, and optical properties of the synthesized PANI materials were analyzed using scanning electron microscopy (SEM), X-ray diffraction (XRD), energy-dispersive X-ray spectroscopy (EDS), Raman spectroscopy, and Fourier transform infrared spectroscopy (FTIR). Results indicated that the synthesized PANI nanoparticles agglomerated into spherical particles with an average size of 70–80 nm. The photocatalytic properties of PANI materials were evaluated by the decolorization of rhodamine B (RhB) and methylene blue (MB) under simulated sunlight irradiation. The PANI photocatalyst was found to be highly effective in removing MB dye, achieving a removal efficiency of approximately 97.09% with a rate constant of 2.08 × 10^{-2} min^{-1}. In comparison, the removal efficiency for RhB was about 58.01%. Additionally, the mechanism behind the photocatalytic degradation of MB dye by PANI was investigated and discussed. The study highlights the photostability and reproducibility of PANI nanoparticles through recycling experiments, contributing to the development of sustainable photocatalytic materials for efficient water treatment.

Received 27th August 2024
Accepted 5th December 2024

DOI: 10.1039/d4na00707g

rsc.li/nanoscale-advances

Introduction

The relentless pursuit of economic advancement and technological progress during the Industrial Revolution has spawned escalating environmental pollution and exacerbated the energy crisis, compelling the imperative for a sustainable future through the progression and enhancement of green and renewable technologies.[1] Industries, including dyeing, food, leather production, electroplating, detonator manufacturing, mining, and pharmaceuticals, discharge wastewater laden with nonbiodegradable, highly toxic, and carcinogenic compounds, such as rhodamine B (RhB), methyl orange (MO), methylene red (MR), acid blue 25 (AB25), metanil yellow (MY), acid orange 7 (AO7) and methylene blue (MB), posing a substantial threat to both the environment and human health.[2] Wastewater treatment, recycling and reuse are effective solutions to address water stress caused by increased consumption, economic development and climate change. Untreated industrial wastewater causes serious pollution, affecting human health and ecosystems, requiring sustainable and technically feasible technologies.[3]

Methods such as bio-oxidation, electrochemical oxidation, advanced oxidation processes (AOPs), and physical and chemical processes are used to remove organic pollutants from the environment. Advanced Oxidation Processes (AOPs) are efficient wastewater treatment methods that employ strong oxidants like hydroxyl ($^{\bullet}OH$) and sulfate ($SO_4^{\bullet-}$) radicals to break down complex organic pollutants, surpassing the limitations of biological treatments. These processes, including photolysis, ozone-based systems, Fenton reactions, and photocatalytic and electrochemical methods, produce reactive species that effectively decompose resistant contaminants into non-toxic byproducts such as CO_2 and H_2O without generating secondary pollution.[4] These systems utilize a diverse range of materials, including polymers, metal oxides, metal sulfides, magnetic materials, carbon-based materials, and various composites.[5,6] Choosing semiconductor photocatalytic oxidation with visible light for organic pollutant treatment is driven

[a]*Institute of Chemistry and Materials, Hanoi, Vietnam. E-mail: duc.duong.la@gmail.com*

[b]*Institute of Materials Science, Vietnam Academy of Science and Technology, Hanoi, Vietnam*

[c]*Institute of Engineering Physics, Hanoi, Vietnam*

[d]*Graduate University of Science and Technology, Vietnam Academy of Science and Technology, Hanoi, Vietnam*

[e]*School of Engineering Physics, Hanoi University of Science and Technology (HUST), Hanoi, Vietnam*

† These authors contributed equally.

by its advanced, eco-friendly nature, overcoming limitations of traditional photocatalysts and enhancing efficacy in wastewater remediation.[7] Researching efficient and stable photocatalysts with visible light responsiveness is a meaningful endeavor. Conducting polymers, including polyaniline (PANI), polythiophene and polypyrrole (PPy), have gained attention as effective adsorbents for aqueous pollutant removal due to their high surface area, tunable morphologies, functional groups, and ease of regeneration.[8,9] Among various adsorbents explored for wastewater treatment, conducting polymers, particularly polyaniline (PANI), have emerged as promising candidates due to their unique combination of properties, including high surface area, excellent conductivity, ease of synthesis, and environmental sustainability.[10]

Polyaniline (PANI) stands out for its ease of synthesis using low-cost monomers, making it a highly attractive material for large-scale applications. Its electrochemical properties, particularly the reversible acid/base redox behavior, lend it high pseudocapacitive performance, which can be effectively utilized in environmental applications such as wastewater treatment and adsorption of harmful contaminants. PANI's unique ability to undergo chemical oxidation and reduction makes it an ideal material for capturing a wide range of pollutants from water, including dyes, heavy metals, and organic compounds. Its high conductivity and electrochemical stability further enhance its suitability for use in adsorption-based water purification systems.[11–13]

The distinctive feature of PANI lies in its capacity to absorb visible light, thereby undergoing a $\pi \rightarrow \pi^*$ electronic transition from the highest occupied molecular orbital (HOMO) to the lowest unoccupied molecular orbital (LUMO), engendering holes (h^+) in HOMO. This process facilitates facile charge separation, enabling efficient photocatalytic activity, particularly in the degradation of organic dyes under visible light, thereby underscoring the commendable suitability of various PANI morphologies for environmentally significant applications.[14]

PANI nanostructures, with enhanced conductivity, stability, and redox properties, show promise in energy-storage devices, sensors, batteries, electrodes, capacitors, molecular electronics, and catalysis.[15,16] Studies have shown that the properties of polyaniline (PANI), such as conductivity, capacitance, catalytic ability, and gas sensitivity, are significantly influenced by its shape and morphology.[17] This relationship between structure and properties is crucial in tailoring PANI for specific applications. For instance, the work of Natalija German *et al.*[18] demonstrates the synthesis of PANI nanoparticles using glucose oxidase (GOx), highlighting the importance of controlling the size and morphology to achieve optimal electrochemical behavior. The detailed characterization of these nanoparticles revealed that their properties could be finely tuned by adjusting the synthesis conditions. Furthermore, Min Seong Cho *et al.*[19] explored the use of different stabilizers, such as polyvinyl alcohol (PVA) and polystyrene sulfonate (PSSA), to synthesize nano-sized PANI particles. They found that PANI–PSSA composites exhibited superior doping levels and conductivity compared to PANI-HCl/PVA, underlining the significant role that morphology and doping level play in enhancing the material's electronic properties. Additionally, the study by Jingping Wang *et al.*[20] reviewed various chemical methods for fabricating one-dimensional nanostructured PANI, such as solid-state polymerization and microwave-assisted techniques. These methods facilitated precise control over the morphology of the material, thereby enabling the development of PANI-based sensors, energy storage devices, and other electronic applications. Moreover, Raju Vivek *et al.*[21] emphasized the biomedical potential of PANI nanoparticles, noting that their size and shape are critical for applications in biosensors, neural probes, and cancer therapy. Similarly, Bakhshali Massoumi *et al.*[22] examined different synthesis techniques, including emulsion and ultrasonic methods, which revealed how variations in solvent, electrolyte, and dopant choice can influence PANI's structure and conductivity. Collectively, these studies underline the vital role of material morphology in determining the performance of PANI in a wide range of applications.

Recent studies have demonstrated the potential of PANI nanostructures in removing contaminants from simulated wastewater. These nanostructures exhibit enhanced adsorption properties, which are influenced by their morphology, surface area, and particle size. For example, research by Ayad *et al.*[15] showed that acid-free synthesized PANI nanoparticles with an average diameter of 20 ± 5 nm demonstrated significantly higher adsorption efficiency for methylene blue compared to conventional PANI powder, with adsorption kinetics fitting the pseudo-second order model. This highlights the importance of optimizing PANI synthesis methods to maximize the material's adsorption potential. Moreover, controlling polymerization parameters such as the APS/aniline ratio, temperature, and reaction time can significantly impact the surface area and conductivity of the final product, as demonstrated by S. Budi *et al.*,[16] who optimized PANI nanoparticles to achieve a surface area of 42.14 $m^2\ g^{-1}$.

Although polyaniline (PANI) has been extensively studied for its effects on size and morphology for applications in energy storage, sensors, batteries, and capacitors, specific studies on pure PANI for high-performance photocatalysis remain limited, especially regarding the role of morphology, surface area, and particle size.[16,23,24]

In this study, PANI nanoparticle structures were successfully synthesized using P123 surfactants *via* the hydrothermal method, followed by calcination. Systematic analyses of crystal structure, micromorphology, and optical properties were undertaken to elucidate the enhanced photocatalytic performance of PANI under visible light irradiation. Rhodamine B (RhB) and methylene blue (MB) were selected to represent toxic, non-biodegradable organic compounds. Superior photocatalytic degradation of MB was observed, achieving approximately 97.09% degradation in 150 minutes under simulated sunlight, compared to about 58.01% for RhB. The photoactivity and regenerability of pure PANI nanoparticles were assessed through photocatalytic recycling experiments.

Results and discussion

Charaterizations of PANI nanoparticle

The morphology and microstructure of the synthesized products were analyzed using SEM, with corresponding data presented in Fig. 1(a and b). The low-magnification SEM image (Fig. 1(a)) reveals a uniform distribution of PANI nanoparticles. Upon closer examination of the high-magnification SEM image (Fig. 1(b)), it is evident that the synthesized PANI nanoparticles agglomerate from spherical particles with an average size of 70–80 nm. In the manufacturing process, the surfactant P123 served as a hard template, providing structural support for uniformly sized nanoparticles. Small, regular nanoparticle sizes are crucial for larger adsorption sites and enhanced photocatalytic performance with organic dyes. This enhancement is attributed to the idea that nanoparticle agglomeration creates a larger specific surface area.[25]

The X-ray diffraction (XRD) spectrum of pure polyaniline (PANI) nanoparticles is presented in Fig. 2(a). The XRD pattern of pristine PANI reveals a prominent broad hump spanning from 10° to 35°. Additionally, a distinctive peak is observed at $2\theta = 25°$, corresponding to the (110) plane of PANI. The observations indicate that the emerald base form of polyaniline (PANI) possesses an amorphous structure, as substantiated by the distinctive peak at $2\theta = 25°$ in the X-ray diffraction (XRD) pattern. This particular peak is attributed to the parallel and perpendicular periodicity of PANI, signifying the amorphous nature of the polymer structure. The presence of this peak in the PANI sample has been corroborated by the Joint Committee on Powder Diffraction Standards (JCPDS) reference code no. 47-2481.[26–28]

EDS analysis of the purified polyaniline (PANI) particles, shown in Fig. 2(c), confirms that the main elements present in the sample are C, N, S, Cl, and O, with no impurities detected. The estimated elemental compositions from the EDS analysis were 72.22% for C, 11.64% for N, 0.26% for S, 0.20% for Cl, and 15.78% for O, verifying the formation of PANI.

Fig. 3 displays the Raman scattering line spectrum of the pure PANI sample, revealing characteristic lines within the 1000 to 1800 cm^{-1} range. The scattering lines at 1180, 1240, 1354, 1470, and 1565 cm^{-1} correspond to specific molecular vibrations in PANI.

The line at 1180 cm^{-1} signifies benzenoid C–H bending in the quinoid ring, while the 1240 cm^{-1} line represents C–N stretching in delocalized polarons. At 1354 cm^{-1}, the semi-quinoid structure of PANI emeraldine salt is evident. The

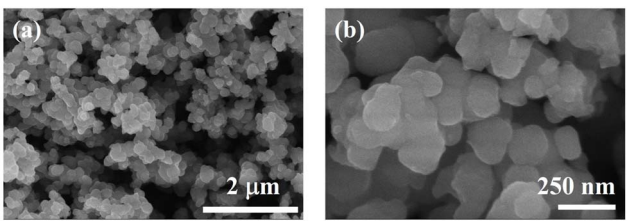

Fig. 1 (a) Low-, (b) high-magnification SEM of the annealed pure polyaniline (PANI).

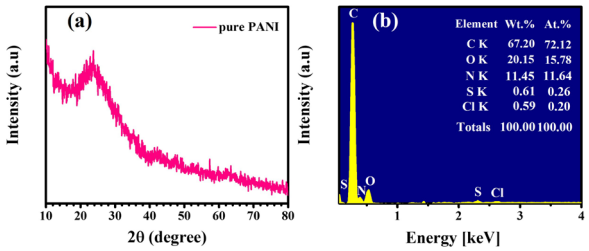

Fig. 2 (a) XRD patterns, and (b) EDS analysis of the pure polyaniline (PANI).

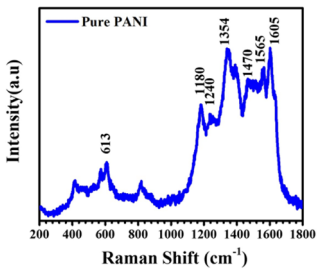

Fig. 3 Raman spectrum of pure PANI nanoparticles.

1470 cm^{-1} line indicates C–C stretching in the benzenoid, and the 1565 cm^{-1} line reflects C═N stretching in the quinoid ring. Additionally, the 1470 and 1565 cm^{-1} lines are associated with $C–N^+$ stretching and C═C stretching vibration modes of the quinoid ring.[29]

Fourier Transform Infrared Spectroscopy (FTIR) was employed to ascertain the functional groups present in the synthesized materials. In Fig. 4, the FTIR spectra of polyaniline (PANI) are depicted. The pristine PANI, as illustrated in Fig. 4, exhibits characteristic absorption bands at 3343 cm^{-1} (N–H band stretching vibration), 1601 cm^{-1} (stretching vibration of the quinoid ring), and 1504 cm^{-1} (stretching vibration of benzene rings). The C–N stretching vibration mode in the aromatic nitro-amine group (quinoid system) of doped polyaniline, detected at 1297 cm^{-1}, indicates its oxidation or protonation state. In-plane vibrations of C–H bending modes in structures, such as N–H stretching, benzene ring vibrations, quinoid ring vibrations, and C–N and C═N groups, are observed at 1173 cm^{-1}. This absorption band indicates the

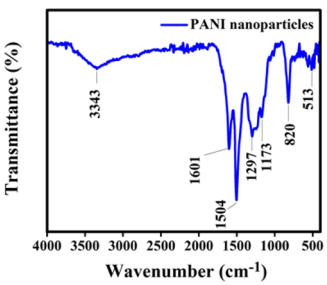

Fig. 4 FT-IR spectra of pure PANI nanoparticles.

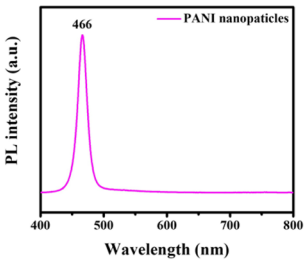

Fig. 5 Photoluminescence (PL) of standard pristine polyaniline nanoparticles.

polymerization of polyaniline (PANI), reflecting the polar structure of its conducting protonated form. The absorption band at 820 cm^{-1} indicates out-of-plane C–H vibrations in a 1,4-disubstituted aromatic ring.[30,31]

The optical properties of pristine polyaniline nanoparticles were investigated by acquiring photoluminescence (PL) spectra at room temperature. A 355 nm excitation wavelength was employed within the wavelength range of 400–800 nm, as illustrated in Fig. 5. In the PL spectrum, pristine polyaniline nanoparticles were identified, demonstrating that the PL intensity peaked at 466 nm. The maximum PL intensity observed at this wavelength indicates efficient radiation recombination within the nanoparticles.[32]

The UV-vis absorption spectrum of pure polyaniline (PANI) nanoparticles, as depicted in Fig. 6(a), shows the primary absorption band spanning from 500 to 800 nm. This absorption band indicates the presence of various electronic transitions within the PANI nanoparticles. The absorption spectrum of PANI displays a weak band at 535 nm, attributed to the p–π* transition from benzenoid to quinonoid rings.[33]

In the analysis, the optical bandgap energy of PANI nanoparticles was determined using ultraviolet-visible diffuse reflectance spectroscopy (DRS). The Kubelka–Munk method, represented by the equation $F(R)h\nu = D(h\nu - E_g)^n$, where $F(R)$ is derived from the diffuse reflectance R using $F(R) = (1-R)^2/2R$, was employed. For PANI nanomaterial, which exhibits a direct bandgap transition, the constant n is taken as 1/2. However, for PANI nanoparticles, the same method can be applied to determine the bandgap energy.

The bandgap of the PANI nanoparticles was determined by plotting $(\alpha h\nu)^{\frac{1}{2}}$ *versus* $h\nu$, where α represents the absorption coefficient and $h\nu$ the photon energy. From this plot, the bandgap energy of PANI nanoparticles was estimated to be 1.36 eV, as shown in Fig. 6(b).

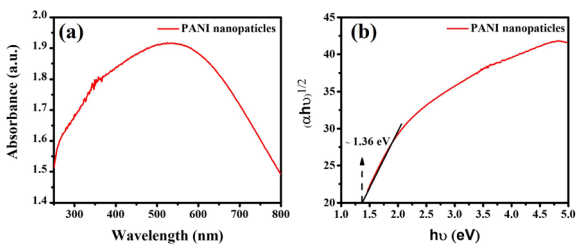

Fig. 6 UV-vis spectra for pure PANI nanoparticles samples (a); respective Tauc plots and estimated band gaps of the synthesized materials (b).

Photocatalytic efficacy of PANI

Research on the photocatalytic performance of pure polyaniline (PANI) nanoparticles was conducted through photodegradation experiments of Rhodamine B (RhB) and methylene blue (MB) dyes under simulated sunlight irradiation (Fig. 7). Fig. 7(a) illustrates the photocatalytic activity of pure PANI nanoparticles towards RhB, where the intensity of the absorption peak at 553 nm was monitored to determine the RhB removal rate. After 210 minutes under visible light, pure PANI nanoparticles exhibited a photocatalytic efficiency of 58.01% in removing RhB. Fig. 7(b) demonstrates that pure PANI nanoparticles effectively degraded 97.09% of MB after 150 minutes of irradiation under simulated sunlight. The absorbance of MB in solution almost completely disappeared, indicating the high photodegradation efficiency of PANI nanoparticles for MB. The degradation rate of MB was calculated to be approximately 2.08 $\times 10^{-2}$ min^{-1}.

The heightened photocatalytic efficacy of pure PANI nanoparticles in MB dye adsorption is attributed to efficient charge separation and distinctive surface morphology. PANI's tunable band gap energy, adsorption capacity, and redox properties contribute to its exceptional performance in MB dye photodegradation, underscoring its potential for enhanced photocatalytic activity through agglomeration reduction.[34,35]

A comparative analysis of methylene blue (MB) photodegradation using various pure polyaniline (PANI) structures, both alone and in combination with metals and other semiconducting metal oxides, is presented in Table 1. This table highlights that pure PANI nanoparticles exhibit notable photocatalytic efficiency, particularly under visible light irradiation, as observed in this and other studies.

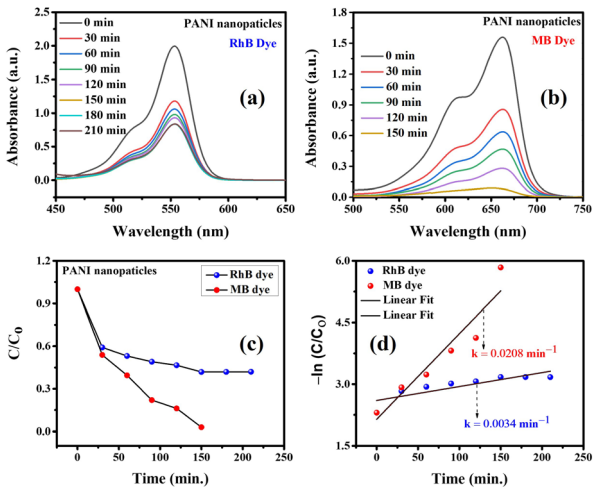

Fig. 7 Effect of photocatalytic time on the removal efficiency of RhB (a) and MB (b); (c) combined adsorption–photodegradation process; and (d) kinetic study of photocatalysts under simulated sunlight irradiation using pure PANI material.

Table 1 Comparison of MB photodegradation efficiency with other catalysts

Photocatalyst	Weight of catalyst	Volume MB of the solution	Initial MB solution concentration	Degradation time (min)	Light source	Photodegradation efficiency (%)	Ref.
PANI nanofibers	50 mg	100 ml	5 mg l^{-1}	105	UV light (Arch lamp housing, model no. 66902) (50–500 W)	42	33
$Ni_{0.2}Fe_{1.8}O_3$/polyaniline	—	—	1×10^{-5} M	50	Visible light	93.2	34
Polyaniline/cellulose/Ni	100 mg	100 ml	0.1 M	55	Tungsten lamp (intensity 500 W)	93	35
Chitosan-polyaniline/ZnS	120 mg	100 ml	25 mg l^{-1}	90	Xenon lamp (250 W)	57.8	36
PANi–NiO	100 mg	100 ml	10 mg l^{-1}	300	Tungsten halogen lamp (500 W)	76	27
PANI/TiO_2	2 ml	100 ml	5 μM	120	Visible light lamps (4 W)	96.2	37
PANI-rGO-MnO_2	20 mg	50 ml	5 mg l^{-1}	120	Halogen bulb (150 W)	90	38
PANI nanoparticles	20 mg	20 ml	10 mg l^{-1}	150	Xenon lamp (350 W)	97.09	This work

Fig. 8 Recyclability of pure PANI nanoparticles photocatalyst for the photodegradation of MB dye.

Reusability and stability assessment of various photocatalysts

One of the important properties of photocatalysts used in practice is their recyclability. In this study, the pure PANI material, after the photocatalytic reaction, could be easily extracted from the solution and reused for multiple MB treatment cycles through centrifugation and thorough washing. The recyclability of the PANI photocatalyst for MB under simulated sunlight irradiation is shown in Fig. 8. The removal efficiency decreased from 97.10% in the first cycle to about 85.61% in the fifth cycle, indicating that the photocatalytic performance of the composite only slightly declined after five cycles. The reduction in removal efficiency by only 11.49% after five cycles demonstrates that pure PANI nanoparticles can be considered sustainable photocatalysts for the treatment of organic dyes in practical applications.

Illuminating the photocatalytic mechanism

The photocatalytic degradation of methylene blue dye with photoactive nanomaterials like polyaniline involves the absorption of visible light, prompting the transition of electrons from the valence band (HOMO) to the conduction band (LUMO). This process induces oxidative and reductive reactions, culminating in the mineralization of adsorbed dye molecules into carbon dioxide (CO_2) and water (H_2O).[39]

Photocatalytic degradation mechanism of MB by PANI nanoparticles under visible light illumination is depicted in Fig. 9. This process involve in generation of electron–hole pairs, and the subsequent separation of these charges is crucial. Electrons in the conduction band react with oxygen to form superoxide anion radicals $O_2^{\bullet -}$, preventing the recombination of electron–hole pairs. Simultaneously, positively charged holes induce the formation of hydroxyl radicals ($OH^{\bullet}$) from water and react with oxygen to produce superoxide anion radicals ($^{\bullet}O_2^{-}$) in the surroundings. These highly reactive species collectively contribute to the efficient degradation and decolorization of MB dye.[14,38,39]

$$\text{PANI} + h\nu \rightarrow \text{PANI}\,(h_{VB}^{+} + e_{CB}^{-})$$

$$h^{+} + H_2O \rightarrow OH^{\bullet} + H^{+}$$

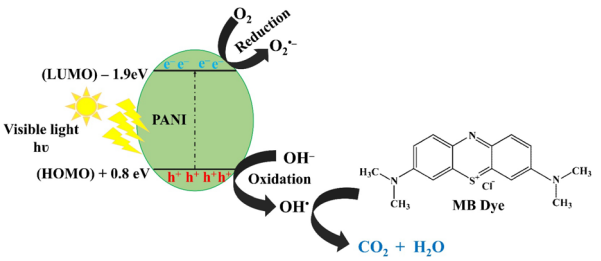

Fig. 9 Photocatalytic degradation mechanism of MB by PANI nanoparticles under visible light illumination.

$$e^- + O_2 \rightarrow O_2^{\bullet -}$$

$$O_2^{\bullet -} + H_2O \rightarrow H_2O_2 \rightarrow 2OH^{\bullet}$$

$$\text{MB dye} + O_2^{\bullet -}/OH^{\bullet} \rightarrow \text{the decomposed colourless products}$$

Conclusions

This study demonstrates the successful synthesis of polyaniline (PANI) nanoparticles *via* a hydrothermal method using P123 surfactants, followed by calcination. The PANI nanoparticles, characterized by SEM, XRD, EDS, Raman spectroscopy, and FTIR, exhibited spherical morphology with an average size of 70–80 nm. The photocatalytic performance of the PANI nanoparticles was assessed through the degradation of rhodamine B (RhB) and methylene blue (MB) under simulated sunlight. The nanoparticles showed superior photocatalytic activity towards MB, achieving a removal efficiency of 97.09% and a rate constant of 2.08×10^{-2} min^{-1}, in contrast to 58.01% removal efficiency for RhB. This significant difference highlights the efficacy of PANI as a photocatalyst for MB degradation. The mechanism of MB degradation by PANI was elucidated, revealing that visible light irradiation generated electron–hole pairs. These charge carriers produced reactive oxygen species, including superoxide anion radicals and hydroxyl radicals, which facilitated the mineralization of MB into non-toxic byproducts. Recycling studies confirmed the stability and reproducibility of the PANI nanoparticles, with a removal efficiency of 85.61% after five degradation cycles, demonstrating their potential for sustainable and repeated use. In conclusion, PANI nanoparticles exhibit remarkable photocatalytic performance, stability, and recyclability, underscoring their potential for use in sustainable water treatment technologies. Further investigation into PANI-based composites could advance the development of high-performance photocatalytic systems for environmental remediation.

Experimental section

Materials

The chemicals used in the study included poly(ethylene glycol)-*block*-poly(propylene glycol)-*block*-poly(ethylene glycol) (P123, ≥99.0%) and ammonium peroxodisulfate ($(NH_4)_2S_2O_8$, ≥98.0%) supplied by Sigma-Aldrich (USA). Absolute ethanol (≥99.8%, AR, 2.5L, CAS: 64-17-5) was obtained from Fisher Scientific (USA). Meanwhile, hydrochloric acid (HCl, 37%), aniline ($C_6H_5NH_2$) were imported from China. All chemicals were of analytical grade and were used directly without purification. Deionized (DI) water was used as a solvent to dissolve chemicals and remove impurities in the experimental procedures.

Synthesis of PANI nanoparticles

Polyaniline nanoparticles were synthesized using a modified hydrothermal method through chemical oxidative polymerization. This approach, unlike the vapor phase method, does not require high temperatures. Aniline, ammonium peroxydisulfate ($(NH_4)_2S_2O_8$), and hydrochloric acid (HCl) were used as precursors, as detailed in our previous study.[40] The protocol for the synthesis of PANI materials is summarized in Fig. 10.

In the experimental procedure, 0.14 mmol of P123 surfactant was added to 80 ml of deionized water in a beaker placed in an ice bath, followed by vigorous stirring for 30 minutes. Subsequently, 0.3 ml of aniline monomer was introduced into the solution with continuous stirring, maintaining a temperature below 5 °C. Simultaneously, 5 ml of HCl acid was added to adjust the pH to approximately ~4, and the solution was stirred for an additional 15 minutes. Following this, 5 mmol of APS was added, resulting in a color change from dense white to a transparent mixture, indicating the progression of aniline polymerization. After thorough stirring within 30 minutes, the solution was transferred to a Teflon-lined stainless-steel autoclave, sealed, and placed in an electric oven for hydrothermal growth at 140 °C for 24 hours. The oven was then turned off, allowing it to cool to room temperature. The product was subjected to centrifugation, washed with deionized water and ethanol separately, and subsequently dried at 60 °C for 2 days under vacuum. The final product underwent heat treatment at 350 °C for 2 hours in an argon.

Characterization

The morphology of the synthesized materials was characterized by Scanning Electron Microscopy (SEM, S-4800, Hitachi) with an Energy-Dispersive X-ray Spectroscopy for elemental analysis. X-ray Diffraction (XRD) was analyzed using an X-Pert Pro (Malvern Panalytical Ltd) with a 1.5418 Å $CuK_{\alpha 1}$ radiation source. Energy dispersive X-ray spectroscopy (EDS, 7395H, Horiba) provided elemental composition data. Raman spectra was studied using

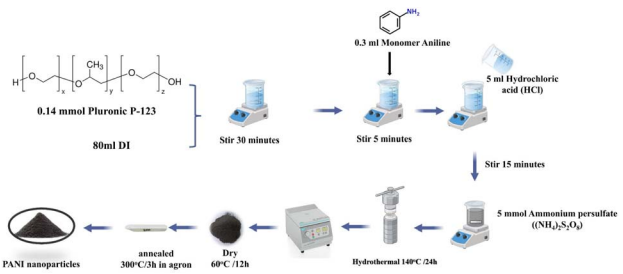

Fig. 10 Process for the hydrothermal synthesis of pure polyaniline (PANI).

InVia confocal micro-Raman Spectroscope (Renishaw) with green laser. Fourier transform infrared spectroscopy (FT/IR-4600, JASCO, Japan) was measured by KBr pellet technique in the range of 400–4000 cm^{-1}. Photoluminescence (PL, iHR550, Horiba) measurements were conducted at 25 °C using an excitation wavelength of 355 nm to evaluate the optical properties. The optical properties of the material were studied using solid-state UV-vis spectroscopy (DRUV-vis, Jasco V-750) and liquid UV-vis absorption spectroscopy (Shanghai Yoke Instrument Co., Ltd, China). Deionized water was used in the experiments. Additionally, the photocatalytic activity of PANI nanoparticles in decomposing RhB and MB dyes was analyzed using a UV-vis spectrophotometer.

Photocatalytic experiment

The photocatalytic performance of the synthesized polyaniline nanoparticle sample was evaluated for methylene blue (MB) and Rhodamine B (RhB) decomposition under visible light. Experiments were conducted in a black irradiation box equipped with a 350 W air-cooled xenon lamp (China, 350 W). In the protocol, 20 mg of PANI material was introduced into two beakers, each containing 20 ml of 10 ppm RhB and MB solutions, respectively. To establish adsorption equilibrium, the mixtures were placed in the dark for 2 hours. After this, the solutions were irradiated with visible light using xenon lamps positioned 15 cm away. At specific time intervals, approximately 3 ml of the solution was withdrawn, centrifuged to remove the catalyst, and analyzed using a UV-vis spectrophotometer. The real-time UV-vis absorption spectra of RhB and MB, at wavelengths (λ_{max}) 553 nm and 664 nm, respectively, were recorded to evaluate the photocatalytic performance of the PANI material in removing RhB and MB.

Data availability

Data for this article, including SEM, XRD, Raman, FTIR, UV-vis, and photocatalytic performance are available at Open Science Framework at **https://osf.io/me67s**.

Author contributions

CVT, DVL: investigation, data collection, writing – original draft preparation. TTN, NQTM: resources, reviewing and editing; HHN, TNM, XQLY: writing – reviewing and editing. DDL: visualization, editing, funding acquisition & supervision. All authors approved the manuscript.

Conflicts of interest

The authors declare that they have no known competing financial interests or personal relationships that could have appeared to influence the work reported in this paper.

Acknowledgements

This work was supported by the staffs and facility at Institute of Chemistry and Materials.

Notes and references

1 S. Sharma, D. Kumar and N. Khare, Hierarchical PANI/CdS nanoarchitecture system for visible light induced photocatalytic dye degradation and photoelectrochemical water splitting, *Polymers*, 2021, **231**, 124117.
2 S. Munusamy, K. Sivaranjan, P. Sabhapathy, P. Ramesh, V. Narayanan, F. Mohammad and S. Sagadevan, Electrochemical and photocatalytic studies of Ta3N5-TaON-PEDOT-PANI nanohybrids, *Chem. Phys. Lett.*, 2021, **780**, 138947.
3 B. J. Singh, A. Chakraborty and R. Sehgal, A systematic review of industrial wastewater management: evaluating challenges and enablers, *J. Environ. Manage.*, 2023, **348**, 119230.
4 Z. U. H. Khan, N. S. Gul, S. Sabahat, J. Sun, K. Tahir, N. S. Shah, N. Muhammad, A. Rahim, M. Imran, J. J. E. Iqbal and E. Safety, Removal of organic pollutants through hydroxyl radical-based advanced oxidation processes, *Ecotoxicol. Environ. Saf.*, 2023, **267**, 115564.
5 A. Enesca and V. Sisman, UV–vis activated CuO/CuS/WO_3@PANI heterostructure for photocatalytic removal of pharmaceutical active compounds, *Ceram. Int.*, 2023, **49**(18), 30592–30602.
6 T. Ahuja, U. Brighu and K. Saxena, Recent advances in photocatalytic materials and their applications for treatment of wastewater: a review, *Journal of Water Process Engineering*, 2023, **53**, 103759.
7 N. Goodarzi, Z. Ashrafi-Peyman, E. Khani and A. Z. Moshfegh, Recent progress on semiconductor heterogeneous photocatalysts in clean energy production and environmental remediation, *Catalysts*, 2023, **13**(7), 1102.
8 A. Samadi, M. Xie, J. Li, H. Shon, C. Zheng and S. Zhao, Polyaniline-based adsorbents for aqueous pollutants removal: a review, *Chem. Eng. J.*, 2021, **418**, 129425.
9 M. F. Banjar, F. N. Joynal Abedin, A. N. S. Fizal, N. Muhamad Sarih, M. S. Hossain, H. Osman, N. A. Khalil, A. N. Ahmad Yahaya and M. Zulkifli, Synthesis and Characterization of a Novel Nanosized Polyaniline, *Polymers*, 2023, **15**(23), 4565.
10 A. Tabasum, H. Razzaq, S. Razzaque, A. Bibi, S. Farooq, A. Yaqub, A. Siddique, T. Amir and S.-u. Rehman, Physics, Protonated polyaniline and its derivatives as potential adsorbents for simultaneous reclamation of textile dyes and oil/water separation, *Mater. Chem. Phys.*, 2023, **293**, 126913.
11 Y. Zhao, M. Arowo, W. Wu and J. Chen, Effect of additives on the properties of polyaniline nanofibers prepared by high gravity chemical oxidative polymerization, *Langmuir*, 2015, **31**(18), 5155–5163.
12 N. Y. Abu-Thabit, Chemical oxidative polymerization of polyaniline: a practical approach for preparation of smart conductive textiles, *J. Chem. Educ.*, 2016, **93**(9), 1606–1611.
13 M. R. Saeb, P. Zarrintaj, P. Khandelwal and N. P. S. Chauhan, Synthetic route of polyaniline (I): conventional oxidative polymerization, in *Fundamentals and Emerging Applications of Polyaniline*, Elsevier, 2019, pp. 17–41.
14 M. Al Kausor and D. Chakrabortty, Polyaniline (PANI) grafted hierarchical heterostructure nanocomposites for

photocatalytic degradation of organic pollutants in waste water: a review, *Surfaces Interfaces*, 2022, **31**, 102079.
15 M. Ayad, G. El-Hefnawy and S. Zaghlol, Facile synthesis of polyaniline nanoparticles; its adsorption behavior, *Chem. Eng. J.*, 2013, **217**, 460–465.
16 S. Budi, A. Juliana, U. Cahyana, A. Purwanto, A. Imaduddin and E. Handoko, Preparation of high surface area and high conductivity polyaniline nanoparticles using chemical oxidation polymerization technique, *J. Phys.: Conf. Ser.*, 2018, 012162.
17 B. Guo, Y. Zhao, W. Wu, H. Meng, H. Zou, J. Chen and G. Chu, Research on the preparation technology of polyaniline nanofiber based on high gravity chemical oxidative polymerization, *Chem. Eng. Process.: Process Intensif.*, 2013, **70**, 1–8.
18 N. German, A. Popov, A. Ramanaviciene and A. Ramanavicius, Evaluation of enzymatic formation of polyaniline nanoparticles, *Polymer*, 2017, **115**, 211–216.
19 M. S. Cho, S. Y. Park, J. Y. Hwang and H. Choi, Synthesis and electrical properties of polymer composites with polyaniline nanoparticles, *Mater. Sci. Eng., C*, 2004, **24**(1–2), 15–18.
20 J. Wang and D. Zhang, One-Dimensional Nanostructured Polyaniline: Syntheses, Morphology Controlling, Formation Mechanisms, New Features, and Applications, *Adv. Polym. Technol.*, 2013, **32**(S1), E323–E368.
21 G. Wang, R. Vivek and J.-Y. Wang, Polyaniline nanoparticles: synthesis, dispersion and biomedical applications, *Mini-Rev. Org. Chem.*, 2017, **14**(1), 56–64.
22 B. Massoumi and R. Mohammadi, Synthesis of nanostructured polyaniline via chemical oxidative polymerization: investigation of morphology and conductivity of the prepared polymers, *Polym. Sci., Ser. B*, 2013, **55**(11), 593–600.
23 X.-W. Lu, W. Wu, J.-F. Chen, P.-Y. Zhang and Y.-B. Zhao, Preparation of polyaniline nanofibers by high gravity chemical oxidative polymerization, *Ind. Eng. Chem. Res.*, 2011, **50**(9), 5589–5595.
24 A. H. Majeed, L. A. Mohammed, O. G. Hammoodi, S. Sehgal, M. A. Alheety, K. K. Saxena, S. A. Dadoosh, I. K. Mohammed, M. M. Jasim and N. U. Salmaan, A review on polyaniline: synthesis, properties, nanocomposites, and electrochemical applications, *Int. J. Polym. Sci.*, 2022, (1), 9047554.
25 J. A. Oyetade, R. L. Machunda and A. Hilonga, Functional impacts of polyaniline in composite matrix of photocatalysts: an instrumental overview, *RSC Adv.*, 2023, **13**(23), 15467–15489.
26 S. Kundu, B. Satpati, T. Kar and S. K. Pradhan, Microstructure characterization of hydrothermally synthesized PANI/$V_2O_5 \cdot nH_2O$ heterojunction photocatalyst for visible light induced photodegradation of organic pollutants and non-absorbing colorless molecules, *J. Hazard. Mater.*, 2017, **339**, 161–173.
27 J. Vidya and P. Balamurugan, Photocatalytic degradation of methylene blue using PANi-NiO nanocomposite under visible light irradiation, *Mater. Res. Express*, 2019, **6**(9), 0950c8.
28 M. L. Dlamini, M. Bhaumik, K. Pillay and A. Maity, Polyaniline nanofibers, a nanostructured conducting polymer for the remediation of Methyl orange dye from aqueous solutions in fixed-bed column studies, *Heliyon*, 2021, **7**(10), e08180.
29 N. S. Al-Kadhi, M. A. Hefnawy, F. S. Alamro, R. A. Pashameah, H. A. Ahmed and S. S. Medany, Polyaniline-supported nickel oxide flower for efficient nitrite electrochemical detection in water, *Polymers*, 2023, **15**(7), 1804.
30 A. B. Rohom, P. U. Londhe and N. Chaure, Enhancement of optical absorption by incorporation of plasmonic nanoparticles in PANI films, *Nanosci. Nanotechnol.*, 2016, **6**, 83–87.
31 B. Qiu, J. Wang, Z. Li, X. Wang and X. Li, Influence of acidity and oxidant concentration on the nanostructures and electrochemical performance of polyaniline during fast microwave-assisted chemical polymerization, *Polymers*, 2020, **12**(2), 310.
32 V. V. Tran, T. T. V. Nu, H.-R. Jung and M. Chang, Advanced photocatalysts based on conducting polymer/metal oxide composites for environmental applications, *Polymers*, 2021, **13**(18), 3031.
33 S. Saha, N. Chaudhary, A. Kumar and M. Khanuja, Polymeric nanostructures for photocatalytic dye degradation: polyaniline for photocatalysis, *SN Appl. Sci.*, 2020, **2**(6), 1115.
34 R. Suresh, K. Giribabu, R. Manigandan, R. Mangalaraja, S. J. Yanez, A. Stephen and V. Narayanan, Synthesis of $Ni_{0.2}Fe_{1.8}O_3$/polyaniline magnetic nanocomposite with excellent photocatalytic activity, *Mater. Lett.*, 2017, **208**, 27–30.
35 N. Ahmad, S. Sultana, G. Kumar, M. Zuhaib, S. Sabir and M. Z. Khan, Polyaniline based hybrid bionanocomposites with enhanced visible light photocatalytic activity and antifungal activity, *J. Environ. Chem. Eng.*, 2019, **7**(1), 102804.
36 P. Sirajudheen, V. R. Kasim, C. Nabeena, M. Basheer and S. Meenakshi, Tunable photocatalytic oxidation response of ZnS tethered chitosan-polyaniline composite for the removal of organic pollutants: A mechanistic perspective, *Mater. Today: Proc.*, 2021, **47**, 2553–2559.
37 Y.-J. Lee, H. S. Lee, C.-G. Lee, S.-J. Park, J. Lee, S. Jung and G.-A. Shin, Application of PANI/TiO_2 composite for photocatalytic degradation of contaminants from aqueous solution, *Appl. Sci.*, 2020, **10**(19), 6710.
38 Y. Park, A. Numan, N. Ponomarev, J. Iqbal and M. Khalid, Enhanced photocatalytic performance of PANI-rGO-MnO_2 ternary composite for degradation of organic contaminants under visible light, *J. Environ. Chem. Eng.*, 2021, **9**(5), 106006.
39 A. Guleria, R. Sharma, A. Singh, N. K. Upadhyay and P. Shandilya, Direct dual-Z-scheme PANI/Ag_2O/Cu_2O heterojunction with broad absorption range for photocatalytic degradation of methylene blue, *J. Water Proc.engineering*, 2021, **43**, 102305.
40 T. T. Nguyet, L. Van Duy, Q. T. M. Nguyet, C. T. Xuan, D. T. T. Le, C. M. Hung, N. Van Duy and N. D. Hoa, Novel synthesis of a PANI/ZnO nanohybrid for enhanced NO_2 gas sensing performance at low temperatures, *J. Electron. Mater.*, 2023, **52**(1), 304–319.